

NASA Contractor Report NASA/CR-2005-211538

Effect of Clouds on Shuttle Imaging

Prepared by:
The Applied Meteorology Unit

Prepared for:
Kennedy Space Center
Under Contract NAS10-01052

NASA
National Aeronautics and
Space Administration

Office of Management

Scientific and Technical
Information Program

2005

Attributes and Acknowledgements

NASA/KSC POC:
Dr. Francis J. Merceret
YA-D

Applied Meteorology Unit (AMU) / ENSCO Inc.
David A. Short
Robert E. Lane, Jr.

Executive Summary

The goal of this study was to determine the effects of clouds on optical imaging of the Space Shuttle launch vehicle (hereinafter the Shuttle) during its ascent from lift-off to Solid Rocket Booster (SRB) separation, by ground based and airborne tracking cameras. This effort was motivated by Recommendation R3.4-1 from the Columbia Accident Investigation Board (CAIB) Report for Space Shuttle return-to-flight that stated: "Upgrade the imaging system to be capable of providing a minimum of three useful views of the space shuttle from liftoff to at least solid rocket booster separation, along any expected ascent azimuth. The operational status of these assets should be included in the launch commit criteria for future launches. Consider using ships or aircraft to provide additional views of the shuttle during ascent."

In response to the CAIB recommendation the Kennedy Space Center (KSC) Weather Office tasked the Applied Meteorology Unit (AMU) to develop a model to forecast the probability that at any time from launch to SRB separation, at least three of the Shuttle ascent imaging cameras will have a view of the Shuttle unobstructed by cloud. Because current observational and modeling capabilities do not permit accurate forecasts of cloud morphology and location, a statistical modeling approach was selected by a team composed of the Shuttle Launch Director, The NASA Intercenter Photo Working Group, the KSC Ice and Debris Team, the KSC Weather Office, the 45th Weather Squadron and the AMU. The AMU formulated a 3-dimensional (3D) model to calculate lines-of-sight from tracking camera locations to the Shuttle during its ascent and to simulate obscuration of the lines-of-sight by an idealized cloud field placed randomly within the 3D domain. Following are the primary elements of the model:

- An ascent trajectory from Space Launch Complex 39B to the International Space Station.
- The network of ground-based cameras prior to a recent upgrade and the network of ground-based and airborne cameras after the upgrade, including 2 airborne cameras.
- 19 basic cloud scenarios with realistic and operationally significant values for cloud base height and cloud thickness, variable horizontal cloud dimensions, fractional cloud cover varying from clear (0) to overcast (8/8) in 1/8 increments and randomized cloud locations.

For each random realization of a cloud field scenario the number of simultaneous views of the Shuttle was determined from the line-of-sight data between lift-off and SRB separation. Then the average percent of time with 3 simultaneous views was computed from 1000 random realizations of each scenario. Analyses of the percent of time viewable were made to determine its sensitivity to cloud amount, cloud base height, cloud thickness, cloud horizontal dimensions, and the upgrade of the camera system.

The results are summarized as follows:

- For overcast conditions the recommendation for at least three simultaneous views could only be met while the Shuttle was below cloud base. For a high overcast of cirrus clouds with bases at 30 000 ft the maximum percent of time viewable would be less than 50%. Broken cloud cover, that is 5/8 to 7/8 coverage, generally would allow 80% or less viewable time, without airborne cameras. When the network includes two airborne cameras the probability of 90% or better time viewable with at least three cameras simultaneously extends from clear conditions up to about 6/8 cloud coverage.
- The impact of upgrading the ground-based network was found to be roughly equivalent to decreasing the cloud cover by about 2/8 in terms of the increased percent of time viewable, except for overcast conditions as noted above. The addition of two airborne cameras was roughly equivalent to decreasing the cloud cover by about 4/8, except for overcast conditions.
- Cloud thickness was the next most important variable with thicker clouds being more efficient at reducing the percent of time viewable. At the typical viewing angles, $< 60^\circ$ above the horizon, the effective cloud cover is increased by the high sides of the clouds. An increase in cloud thickness from 500 ft to 5000 ft was roughly equivalent to increasing the fractional cloud cover by 1/8 to 2/8.

The AMU also mapped out the geographic boundaries of the domain where clouds could potentially obscure imagery of the Shuttle from individual cameras within the network. This product could be used to provide subjective operational guidance to the Shuttle Launch Weather Officer regarding the susceptibility of various camera sites to cloud obscuration in real-time, if it were developed into an overlay for satellite imagery.

Table of Contents

| | |
|---|-----|
| Executive Summary | iii |
| List of Tables..... | vii |
| 1. Introduction | 1 |
| 1.1 Purpose of Memorandum | 1 |
| 1.2 AMU Shuttle Imaging Weather Evaluation Concept Study | 1 |
| 1.3 Rationale for at least N Simultaneous Views | 2 |
| 1.4 Approach of this Study | 2 |
| 2. Camera Locations, Shuttle Ascent Trajectory, and Lines-of-Sight | 3 |
| 2.1 Camera Network..... | 3 |
| 2.1.1 Short-Range Cameras | 3 |
| 2.1.2 Medium-Range Cameras | 3 |
| 2.1.3 Long-Range Cameras | 5 |
| 2.2 Ascent Trajectory | 8 |
| 2.3 Lines-of-Sight and Cloud Obscuration Zones | 9 |
| 3. Simulation Model..... | 11 |
| 3.1 Coordinate System..... | 12 |
| 3.2 Cloud Scenarios..... | 12 |
| 3.3 Method of Solution..... | 14 |
| 3.4 Model Output..... | 14 |
| 4. Analysis Results | 16 |
| 4.1 Probability of at least 3 Simultaneous Views with Upgraded Camera Network | 16 |
| 4.1.1 Sensitivity to Cloud Base Height..... | 17 |
| 4.1.2 Sensitivity to Cloud Thickness | 18 |
| 4.1.3 Sensitivity to Cloud Horizontal Dimension..... | 19 |
| 4.1.4 Sensitivity to Cloud Layering..... | 20 |
| 4.2 Comparison of Post- and Pre- Upgraded Networks..... | 21 |
| 5. Summary | 23 |
| 5.1 Objective..... | 23 |
| 5.2 Camera Network, Ascent Trajectory and Line-of-Sight data | 23 |
| 5.3 Simulation Model and Cloud Scenarios | 24 |
| 5.4 Results | 24 |
| 5.5 Future Work..... | 24 |
| 6. Bibliography..... | 25 |

List of Figures

| | | |
|------------|--|----|
| Figure 1. | Hierarchy of potential methodologies showing increased capability with time... .. | 2 |
| Figure 2. | A) Pre-upgrade configuration of the medium-range camera sites. B) Post-upgrade configuration of medium range camera sites..... | 5 |
| Figure 3. | Pre-upgrade configuration of the long-range camera sites. | 7 |
| Figure 4. | Post-Upgrade configuration of the long-range camera sites..... | 8 |
| Figure 5. | Time/height cross section of the ascent of STS-108 from lift-off to SRB separation..... | 9 |
| Figure 6. | Azimuth/elevation cross section of a Shuttle launch trajectory as viewed from UCS-3..... | 9 |
| Figure 7. | Schematic view of the lines-of-sight from a camera site in the upper left-hand corner to a Shuttle along its ascent trajectory from lift-off at the launch site to SRB separation at 155 000 ft above the Earth's surface. | 10 |
| Figure 8. | Geographical pattern of camera zones susceptible to cloud obscuration for the upgraded long-range camera network with cloud bases at 3000 ft and cloud tops at 27 000 ft. | 11 |
| Figure 9. | Schematic of the model coordinate system used for the imaging simulations..... | 12 |
| Figure 10. | Cloud horizontal scale versus cloud bases and tops for 19 basic cloud scenarios used in the simulations of cloud effects on Shuttle imaging..... | 13 |
| Figure 11. | Fractional cloud cover versus percent of time between lift-off and SRB separation that the Shuttle was viewable simultaneously by at least 1, 2 and 3 cameras. | 17 |
| Figure 12. | Fractional cloud cover versus percent of time from lift-off to SRB separation that the Shuttle was viewable simultaneously by at least 3 cameras for cloud bases at 4000, 8000, and 30 000 ft..... | 18 |
| Figure 13. | Fractional cloud cover versus percent of time between lift-off and SRB separation that the Shuttle was viewable simultaneously by at least 3 cameras for cloud bases at 8000 ft and cloud thicknesses of 500 ft and 5000 ft. | 19 |
| Figure 14. | Fractional cloud cover versus percent of time between lift-off and SRB separation that the Shuttle was viewable simultaneously by at least 3 cameras for cloud bases at 8000 ft, cloud thicknesses of 500 ft and cloud horizontal dimensions of 1, 4, and 8 n mi. | 20 |
| Figure 15. | Fractional cloud cover versus percent of time between lift-off and SRB separation that the Shuttle was viewable simultaneously by at 3 cameras for two cases: Cloud bases at 8000 ft, cloud thicknesses of 500 ft and cloud horizontal dimensions of 4 n mi (thin line), and cloud layers at 8000' and 30 000 ft with the same thicknesses and horizontal dimensions..... | 21 |
| Figure 16. | Fractional cloud cover versus percent of time between lift-off and SRB separation that the Shuttle was viewable simultaneously by at least 3 cameras for the pre-upgrade network (Δ), the post-upgrade network without airborne cameras (O), and the post-upgrade network with airborne cameras (*), for cloud bases at 8000 ft, and cloud thicknesses of 500 ft. | 22 |
| Figure 17. | Fractional cloud cover versus percent of time between lift-off and SRB separation that the Shuttle was viewable simultaneously by at least 3 cameras for the pre-upgrade network (Δ), the post upgrade network without airborne cameras (O and o), and the post-upgrade network with airborne cameras (* and *), for cloud bases at 8000 ft, and cloud thicknesses of 500 ft. The small symbols denote a change in the post-upgrade configuration from 10 to 8 long-range cameras. | 23 |

List of Tables

Table 1. Medium Range Camera Sites.....4

Table 2. Long range Camera Sites.....6

Table 3. Sample Model Output..... 15

1. Introduction

1.1 Purpose of Memorandum

This Applied Meteorology Unit (AMU) report documents the findings from AMU simulations depicting the effects of clouds on optical imaging of the Space Shuttle launch vehicle (hereinafter the Shuttle) from lift-off to Solid Rocket Booster (SRB) separation. The computer simulations included 1) idealized, random cloud coverage scenarios, 2) optical lines-of-sight from optical imagers to the Shuttle using the camera network before and after upgrades for Return-to-Flight (RTF) and 3) a Shuttle ascent trajectory for a launch from Space Launch Complex 39B to the International Space Station (ISS). Descriptions of the camera network before and after upgrade and of the simulation model are also provided, along with analyses of the probability of at least 3 simultaneous views.

1.2 AMU Shuttle Imaging Weather Evaluation Concept Study

In September 2003, the AMU was tasked by the NASA Kennedy Space Center (KSC) Weather Office to: *"Identify and evaluate alternative methods for determining whether or not a sufficient number of Shuttle launch imaging cameras will have a field of view unobstructed by weather."* At that time, the KSC Weather Office advised that the forecast guidance should be available at the end of the T-9 minute hold and be valid throughout the 5-minute launch window for ISS missions. The lifetimes of individual cloud elements capable of obscuring optical views of the Shuttle are typically 20 minutes or less, posing an unprecedented challenge for observing and forecasting cloud obscuration over an extended network of cameras. The Weather Office advised that although a firm Go/No-Go indicator was highly desirable, a probabilistic assessment would be acceptable if a binary indicator was impossible to develop. In October 2003 the AMU concluded a Concept Study (Bauman 2003) that outlined two complementary methodologies: statistical and observational, as shown in Figure 1 (Fig. 4 from Bauman 2003). The Concept Study recommended that since even the best numerical simulations based on real observations will never reach "Truth", it would be prudent to incorporate statistical results into the forecast guidance.

After a review of the AMU Concept Study by a team consisting of the Shuttle Launch Director, The NASA Intercenter Photo Working Group, the KSC Ice and Debris Team, the KSC Weather Office, the 45th Weather Squadron (45 WS) and the AMU, the statistical methodology schematically represented on the left side of Figure 1 was selected for further development.

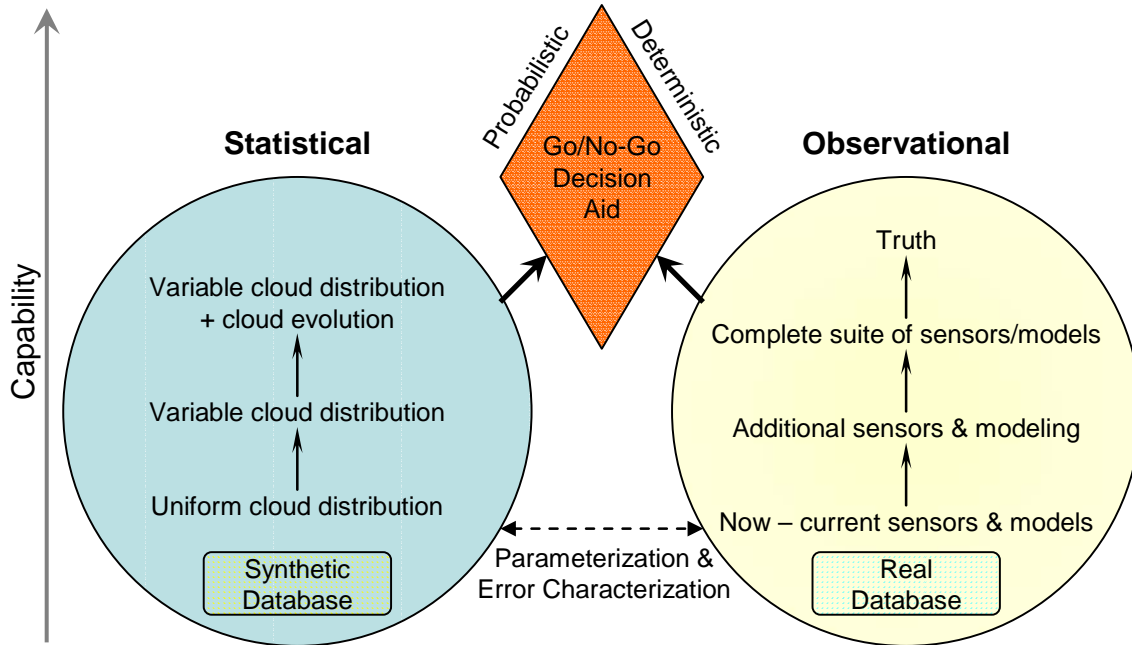


Figure 1. Hierarchy of potential methodologies showing increased capability with time. A statistical method is represented by the circle on the left which illustrates increasing levels of complexity to simulate cloud fields. The statistical method could provide earliest capability for a Go/No-Go Decision Aid, if required, as a probabilistic tool. An observational method, represented by the circle on the right, illustrates increased capability gained through improved sensors and numerical simulations and modeling of near real-time data. The observational method has the potential to provide a more deterministic tool for a Go/No-Go Decision Aid, if required (From Bauman 2003, Fig. 4).

1.3 Rationale for at least 3 Simultaneous Views

In November 2003 the Weather Office tasked the AMU to: *“Develop a model to forecast the probability that at any time from launch to SRB separation, at least three of the Shuttle ascent imaging cameras will have a view of the vehicle unobstructed by cloud.”* This task was motivated by Recommendation R3.4-1 from the Columbia Accident Investigation Board (CAIB) Report (NASA 2003) for Space Shuttle RTF that stated: *“Upgrade the imaging system to be capable of providing a minimum of three useful views of the space shuttle from liftoff to at least solid rocket booster separation, along any expected ascent azimuth. The operational status of these assets should be included in the launch commit criteria for future launches. Consider using ships or aircraft to provide additional views of the shuttle during ascent.”*

Although Figure 1 shows the statistical and observational methodologies converging on a Go/No-Go decision aid, further guidance from the Launch Director emphasized that the use of ground camera imagery is for “quick-look” and post flight data analysis. The ground-based cameras are not a flight safety asset and true assessment of orbiter damage will come from on-orbit assets. For those reasons this study focused on the probability of achieving at least 3 simultaneous views, for various configurations of the imaging network and various randomized cloud coverage scenarios.

1.4 Approach of this Study

In order to provide a quantitative assessment of the risk that clouds would obscure optical imagery of the Shuttle, the approach taken was in the spirit of a probabilistic risk analysis (Pate-Cornell and Fischbeck 1994). A computer simulation model was used to estimate the ability that a network of optical imaging cameras would obtain at least 3 simultaneous views of the Shuttle from lift-off to SRB separation in the presence of clouds. The model generated line-of-site (LOS) data for a defined camera network and Shuttle

ascent trajectory. The camera network and ascent trajectory were embedded in a 3-dimensional (3D) field of randomly distributed clouds. The LOS from each camera to the Shuttle was computed along its trajectory and cloud obscuration was noted as a binary variable, either obscured or clear. The obscuration data was then analyzed to determine the fraction of time from liftoff to SRB separation that at least 3 simultaneous views of the Shuttle were obtained by the camera network. A total of 1000 trials with randomly distributed clouds was analyzed for each of approximately 19 different cloud scenarios. The cloud scenarios had prescribed cloud bases, tops and widths, with cloud coverage ranging from 1/8 to 7/8s.

2. Camera Locations, Shuttle Ascent Trajectory, and Lines-of-Sight

The sequence of elevation and azimuth angles followed by each tracking camera during a Shuttle launch is determined by the Shuttle trajectory and the camera location. These factors combine to determine the susceptibility of each camera to obscuration by clouds, which depends on cloud characteristics such as location, altitudes of base and top, and size. This section provides details of the camera locations and Shuttle trajectory used for determining LOS sequences for each camera.

2.1 Camera Network

Characteristics of the camera network were obtained from Mr. Robert Page, Chair of the Intercenter Photo Working Group (IPWG) at NASA/KSC, and Mr. Robbie Robinson, a member of the IPWG. The required characteristics for the study were confined to camera locations and the portion of the ascent trajectory where high resolution imagery of the Shuttle that are useful for “quick look” and post flight data analyses can be obtained by each camera type. Brief descriptions of the camera types and locations follow. More details on the camera network can be found in Bauman (2003).

2.1.1 Short-Range Cameras

There are numerous short-range tracking cameras located around the Shuttle launch pads. These provide high-resolution imagery from a few seconds before lift-off until the Shuttle reaches about 1200 ft to 1500 ft in altitude, approximately 11 to 13 seconds after lift-off. The short-range cameras were not included in the simulation results presented here because the cloud coverage scenarios did not include clouds with bases below 1500 ft. It was assumed that the short-range tracking cameras provided the required views of the Shuttle for this early portion of the ascent in both the pre- and post-upgrade configurations. This assumption also made it unnecessary to take into account camera obscurations by buildings and trees and over the horizon effects during the first few seconds of the ascent.

2.1.2 Medium-Range Cameras

Table 1 lists the medium-range camera locations in the pre- and post-upgrade configurations. Universal Camera Sites are denoted by UCS. It was assumed that the medium-range cameras picked up where the short-range cameras left off in acquiring imagery. It was further assumed that the medium range cameras could acquire useful imagery in the absence of cloud obscuration, until the Shuttle reached about 7000 ft in altitude, ~ 26.1 seconds after lift-off and 21% of the time from lift-off to SRB separation.

Table 1. Medium Range Camera Sites used in simulations for the pre- and post-upgrade networks. The site name, latitude and longitude are listed. Each site is denoted as north or south as explained in the text below.

| Site Name | Latitude | Longitude | Pre-Upgrade | Post-Upgrade |
|------------------|----------|-----------|-------------|--------------|
| N. Beach J8-1821 | 28.60702 | -80.5939 | South | South |
| Site B SLF | 28.61507 | -80.6926 | North | North |
| UCS-5 | 28.64416 | -80.6656 | North | North |
| UCS-7 | 28.62159 | -80.6075 | South | South |
| UCS-9 | 28.66364 | -80.6388 | | North |
| UCS-10 | 28.70312 | -80.6680 | North | North |
| UCS-15 | 28.57816 | -80.6084 | South | South |
| UCS-17 | 28.60195 | -80.6403 | | South |

The medium-range camera sites in Table 1 were listed as north or south depending on whether their view of the ascent trajectory was from the north or south side of the ascending Shuttle. After the Shuttle completes its roll maneuver about 10 seconds after lift-off, the right side of the Shuttle (designated + Y) is viewable from the north side cameras, while the left side of the Shuttle (designated -Y) is viewable by the south side cameras.

Figure 2 shows the medium range cameras before and after upgrade along with the ground track of the ascent trajectory for an ISS mission (STS-108), out to ~26.1 seconds.

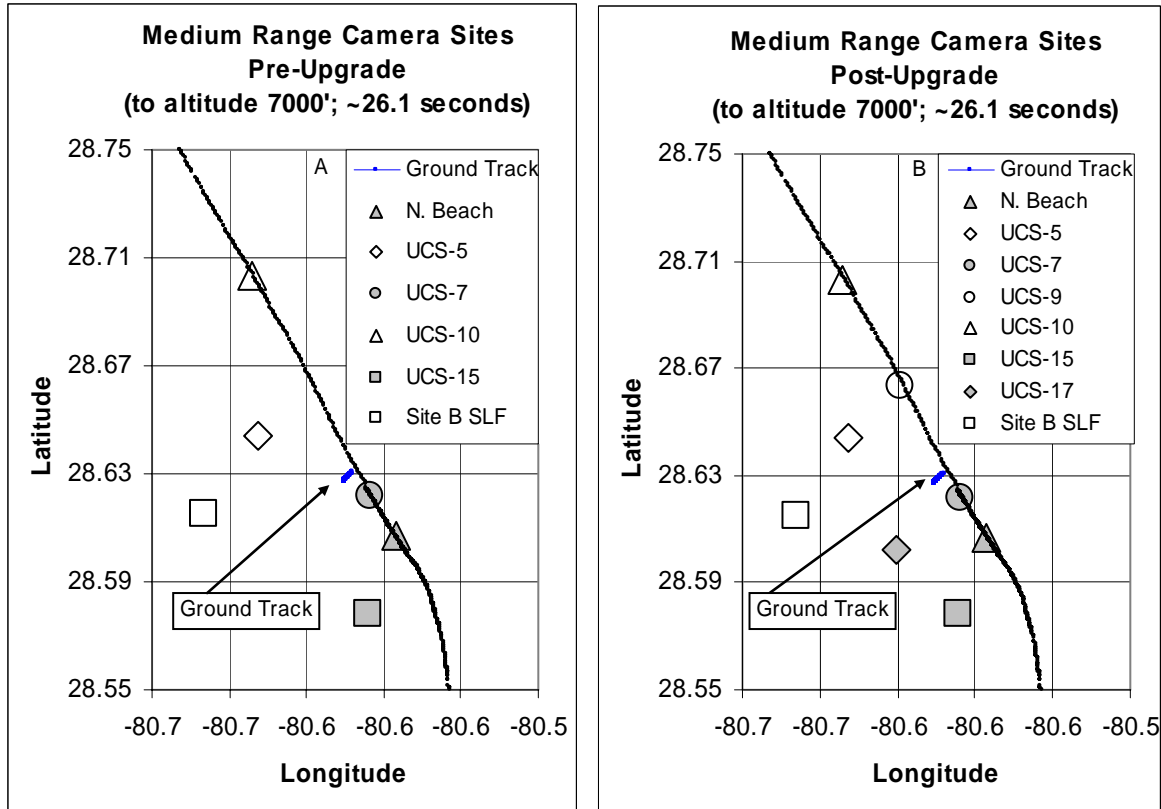


Figure 2. A) Pre-upgrade configuration of the medium-range camera sites. B) Post-upgrade configuration of medium range camera sites. The ground track of the Shuttle from lift-off to ~ 26.1 seconds is shown by the short line segment near the middle of the figure.

2.1.3 Long-Range Cameras

Table 2 lists the long-range cameras in the pre- and post-upgrade configurations used for this simulation study. There were three assumptions made regarding the operating parameters of the long-range cameras. The first was that the long-range cameras picked up where the medium-range cameras left off, in terms of acquisition of useful imagery. The second assumption was that the long-range cameras could acquire useful imagery, in the absence of cloud obscuration, until the Shuttle reached SRB separation at an altitude of about 155 000 ft, ~ 124 seconds after lift-off. Finally, it was assumed that the airborne cameras, stationed at 65 000 ft altitude 15 n mi northwest and southeast of the SRB separation point could acquire imagery from lift-off to SRB separation.

The long-range camera sites were also denoted as N or S in Table 2 depending on whether their view of the Shuttle was from the north or south side. The asterisks for sites UCS-1 and UCS-25 in Table 2 indicate that UCS-1 was used in an initial upgraded configuration without site UCS-25, and that in the final upgraded configuration UCS-1 was dropped and UCS-25 was added.

| Table 2. Long Range Camera Sites used in simulations for the pre- and post-upgrade networks. The site name, latitude and longitude are listed. Each site is denoted as north or south as explained in the text following Table 1. | | | | |
|---|----------|-----------|-------------|--------------|
| Site Name | Latitude | Longitude | Pre-Upgrade | Post-Upgrade |
| Aircraft 1 | 28.72308 | -80.0495 | | S |
| Aircraft 2 | 29.13856 | -80.3839 | | N |
| Apollo Beach | 28.85772 | -80.7762 | | N |
| Cocoa Beach | 28.35138 | -80.6061 | S | S |
| LC-46 | 28.45849 | -80.5284 | | S |
| PAFB | 28.22704 | -80.5996 | S | |
| Playalinda Beach | 28.70288 | -80.6686 | N | N |
| Ponce Inlet | 29.06700 | -80.9130 | | N |
| Shiloh | 28.81950 | -80.8370 | N | N |
| UCS-1 | 28.46427 | -80.6504 | | S* |
| UCS-3 | 28.57512 | -80.5736 | | S |
| UCS-11 | 28.68685 | -80.7190 | | N |
| UCS-23 | 28.50342 | -80.5590 | S | S |
| UCS-25 | 28.43673 | -80.5676 | | S* |

Figure 3 shows the long-range cameras before upgrade along with the ground track of the ascent trajectory for an ISS mission, out to SRB separation.

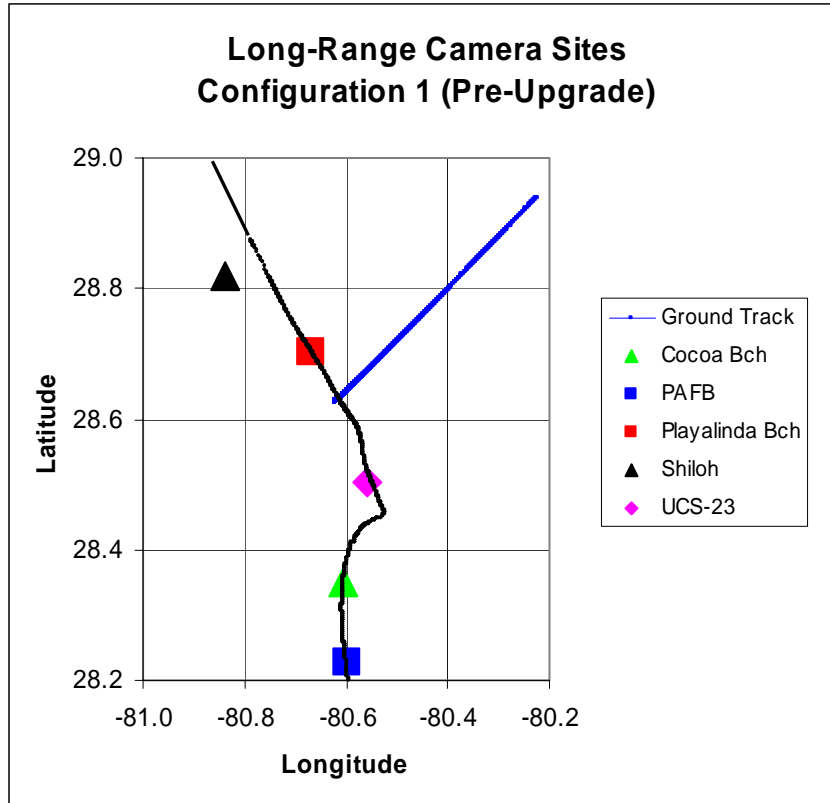


Figure 3. Pre-upgrade configuration of the long-range camera sites. The ground track of the Shuttle from lift-off to SRB separation is shown by the line projecting toward the upper-right.

Figure 4 shows the long-range cameras after upgrade along with the ground track of the ascent trajectory for an ISS mission, from launch to SRB separation. Note that there were 5 ground-based camera sites on the north and south sides, taking into account the switch from UCS-1 to UCS-25.

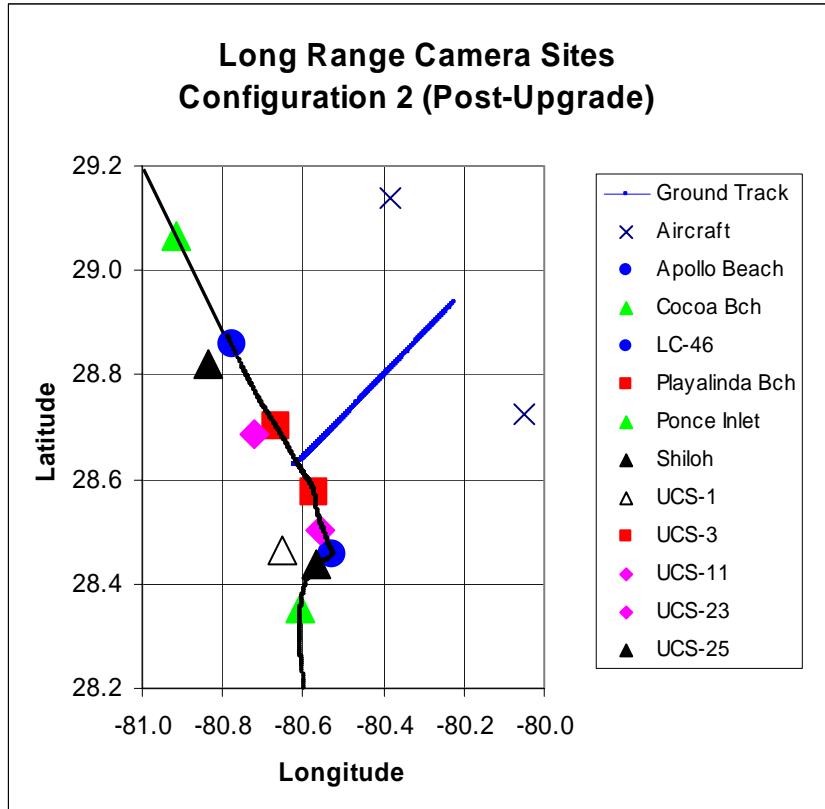


Figure 4. Post-Upgrade configuration of the long-range camera sites. The initial upgraded configuration was with site UCS-1 and without site UCS-25. The final upgraded configuration dropped UCS-1 and added UCS-25. The airborne cameras are located 15 n mi NE and SW of the SRB separation point at an altitude of 65 000 ft.

2.2 Ascent Trajectory

Figure 5 shows a time-height cross section of the Shuttle ascent trajectory used in the present simulation study. Latitude, longitude and altitude points at 0.1 second intervals were obtained for STS-108, an ISS mission with a 56.1° azimuth (toward the north-east). The ground track of ascent is shown in Figures 3 and 4. The timeline in Figure 5 covers 124.2 seconds from lift-off to SRB Separation.

Figure 5 also shows that the Shuttle passed through the 50 000 ft level after about 70 seconds of ascent, which is 56% of the time from lift-off to SRB separation. The 50 000 ft level is meteorologically significant as it corresponds to the average height of the tropopause in the KSC/CCAFS area and a practical upper limit to the height at which clouds can be expected during a launch. Although the Shuttle is likely to be above all clouds after 70 seconds, clouds within the troposphere would have the potential to obscure views from tracking cameras throughout the entire 124.2 second time period if the clouds were in the line-of-sight between a camera and the Shuttle.

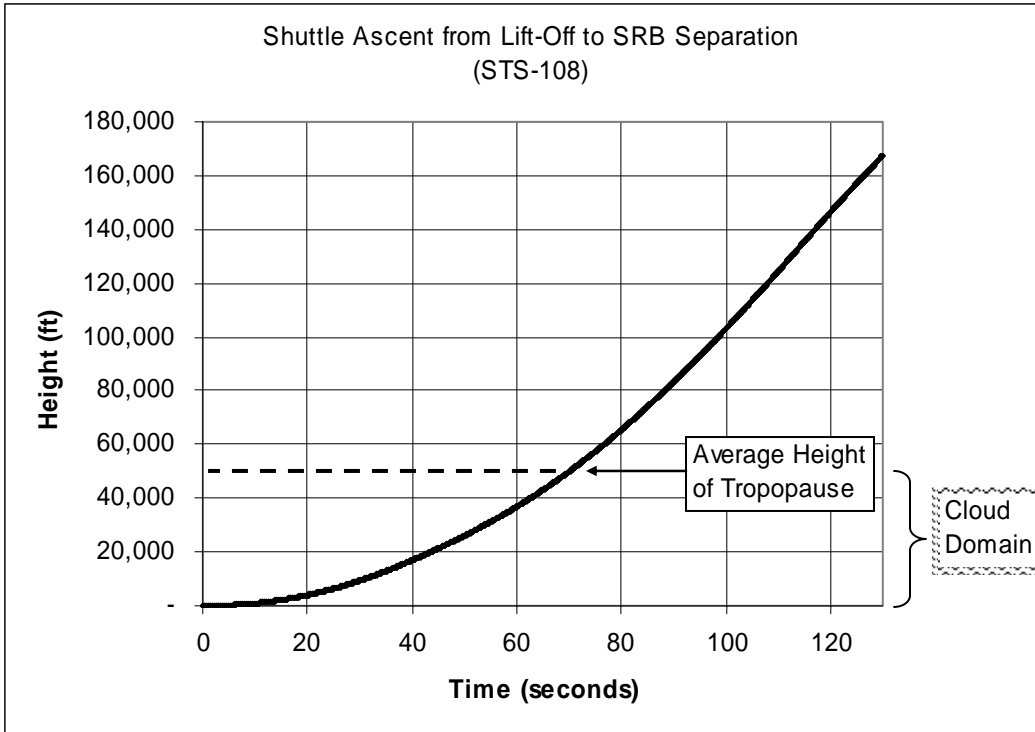


Figure 5. Time/height cross section of the ascent of STS-108 from lift-off to SRB separation. The average height of the tropopause is shown near a height of 50 000 ft. Clouds that could affect optical imaging of the Shuttle would most likely occur within the troposphere, below the tropopause.

2.3 Lines-of-Sight and Cloud Obscuration Zones

The line-of-sight from a tracking camera to the Shuttle sweeps across the sky as the Shuttle travels along its ascent trajectory. Figure 6 shows a 2-dimensional cross section of the azimuth and elevation angles that would be followed by a camera at UCS-3 as it moved across the sky tracking the Shuttle. Earth curvature effects are evident at the SRB separation point as the elevation angle is decreasing, even though the Shuttle continues to ascend.

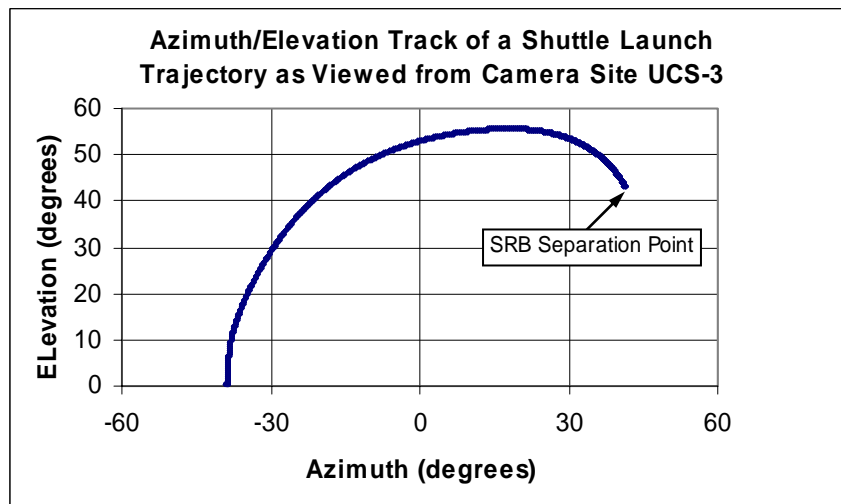


Figure 6. Azimuth/elevation cross section of a Shuttle launch trajectory as viewed from UCS-3.

Figure 7 shows an imaginary 3D surface made up of sequential lines-of-sight from a camera (upper left) to the Shuttle from lift-off to SRB separation at 155 000 ft. The 3D surface is divided into regions A, B and C, where the boundaries have been determined by a cloud base altitude (CB) and a cloud top altitude (CT). If cloud elements were present within region C they would obscure the line-of-sight from the camera to the Shuttle sometime during its ascent. Similar cloud elements within region A could not obscure the view as the line-of-sight would pass beneath them during the portion of the ascent from lift-off until the Shuttle reached cloud base. In a similar manner cloud elements in region B could not obscure the line-of-sight as the Shuttle would be above them and they would be too far from the camera site.

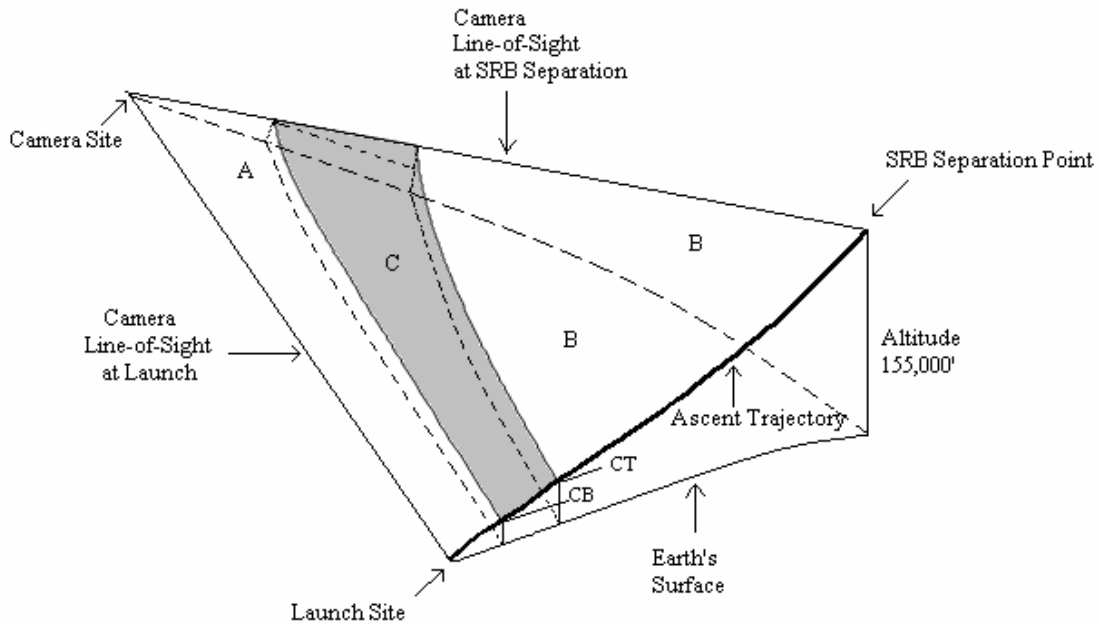


Figure 7. Schematic view of the lines-of-sight from a camera site in the upper left-hand corner to a Shuttle along its ascent trajectory from lift-off at the launch site to SRB separation at 155 000 ft above the Earth’s surface. Regions A, B and C comprise a 3-dimensional surface of the lines-of-sight from the camera to the Shuttle along its ascent trajectory. Region C is the domain where cloud elements with bases at altitude CB and tops at altitude CT have the potential for obscuring the line-of-sight from the camera to the Shuttle during its ascent.

The geographic boundaries of the domain labeled C in Figure 7 can be computed for any camera site and any prescribed CB and CT. Figure 8 shows a composite of the zones susceptible to cloud obscuration for the post-upgrade long-range camera network shown in Figure 4 with CB at 3000 ft and CT at 27 000 ft. This cloud scenario was selected from the simulations described in Section 3 and could be representative of late morning convective elements during the warm season (May – September) or frontal clouds during the cool season (October – April). The zones susceptible to cloud obscuration shown in Figure 8 are mostly off-shore and are confined to within less than 10 n mi of the coast.

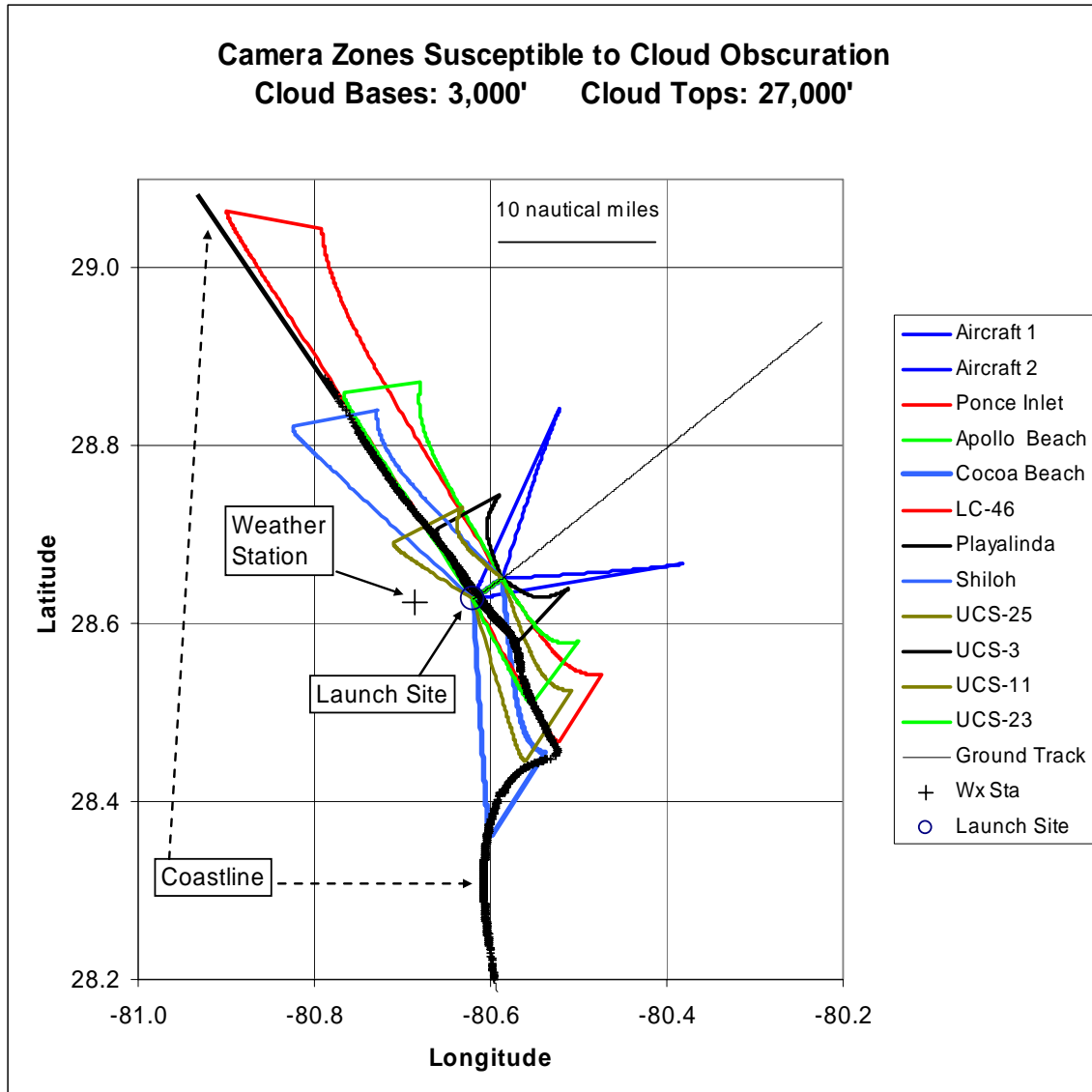


Figure 8. Geographical pattern of camera zones susceptible to cloud obscuration for the upgraded long-range camera network with cloud bases at 3000 ft and cloud tops at 27 000 ft. The weather station near the Shuttle runway (+) is where routine surface-based observations of cloud height and cloud amount are obtained.

The complex geographical pattern shown in Figure 8 provides an indication of the difficult challenges that would have to be overcome in order to provide an accurate forecast of the effect of clouds on viewing conditions from a network of cameras. Although it may be possible to diagnose an existing cloud geometry over the region with advanced instrumentation such as cloud radars, cloud lidars and high-resolution satellite observations (Bauman 2003), an accurate 15-minute forecast of the cloud geometry would be beyond the present state-of-the art.

3. Simulation Model

As stated earlier, the KSC Weather Office tasked the AMU to use statistical methods to estimate the probability of obtaining at least 3 simultaneous views of the Shuttle from a network of cameras, with prescribed cloud bases tops and sky coverage, but random cloud locations. The simulation model used for computing the probabilities is described in this section.

3.1 Coordinate System

The model was executed in 3D Earth Centered Earth Fixed (ECEF) coordinates on an oblate spheroidal earth. Figure 9 shows a schematic of the model coordinate system. Clouds were represented as 6-sided rectangles with faces parallel to lines of latitude, longitude, and the earth's tangent plane below each cloud. Camera sites, including airborne cameras were fixed (See Tables 1 and 2). The Shuttle position was represented at 0.1-second intervals from lift-off to SRB separation.

In Figure 9 the LOS from a ground based camera (O) to the Shuttle (S) passes through a cloud element centered at $(x_1+x_2)/2$, $(y_1+y_2)/2$ and $(z_1+z_2)/2$. The cloud elements have defined bases (z_1), tops (z_2), and horizontal dimensions, as described below.

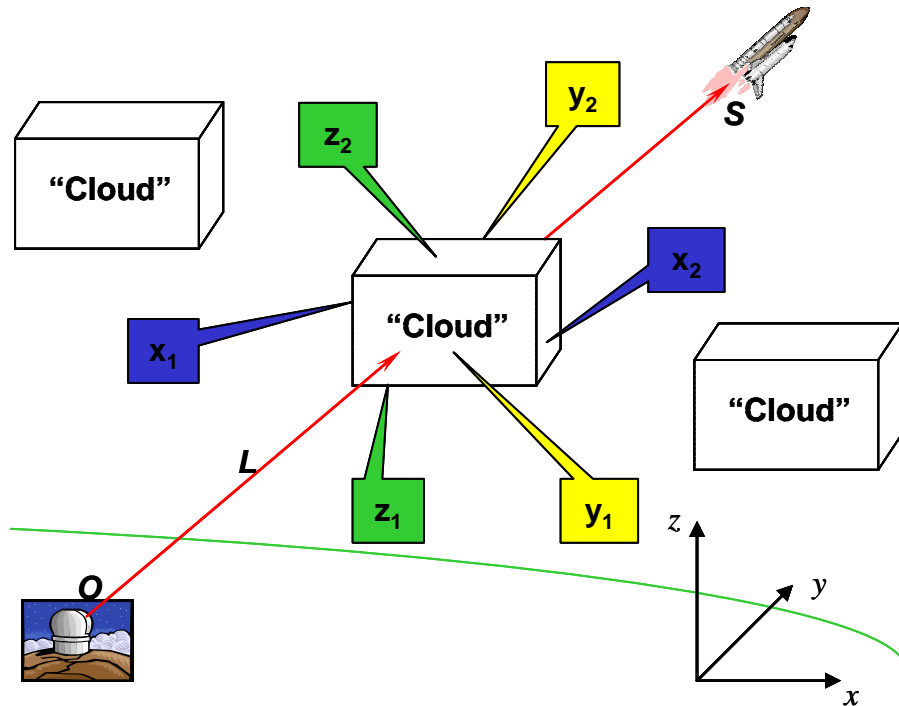


Figure 9. Schematic of the model coordinate system used for the imaging simulations. The line-of-sight between a ground-base camera (O) and the Shuttle (S) intersects a cloud with base and top at Z_1 and Z_2 , while the north-south and east-west boundaries are located at Y_2 , Y_1 and X_2 , X_1 , respectively. The Earth's limb is represented by the curved line between the camera site and the cloud.

3.2 Cloud Scenarios

The model domain extended 64 n mi in the north-south and east-west directions in order to represent the extent of the camera network, the ground track of the Shuttle, and the domain where cloud elements could obscure camera views of the Shuttle (see Fig. 8). The domain was divided into cells with horizontal dimensions of 1, 2, 4, 8 or 16 n mi., depending on the cloud scenario to be simulated. For the cases with cloud horizontal dimensions of 32 n mi, the model domain was extended to 128 x 128 n mi. Vertical faces of cloud elements corresponded to cell boundaries. The cell location of each cloud element, between X_1 and X_2 , and Y_1 and Y_2 , was randomly assigned.

Figure 10 shows 19 cloud scenarios selected to provide estimates of viewing probabilities over a range of conditions that could be expected to impact launch conditions over coastal east-central Florida. For each scenario a cloud base and cloud top were selected along with a range of horizontal scales. Cloud coverage was varied from 0/8 to 8/8, and was defined as the fraction of cells within the model domain that were assigned as cloudy.

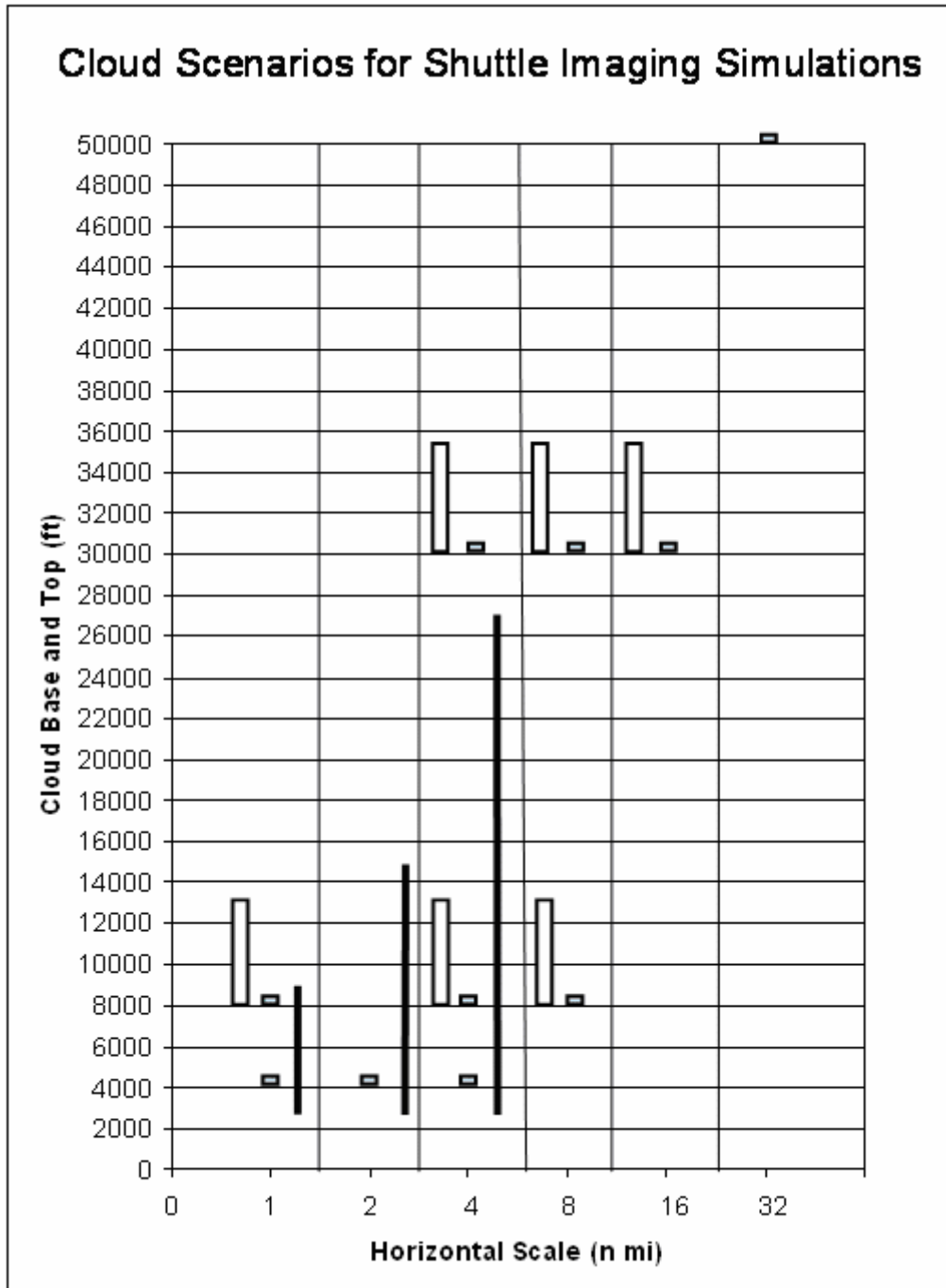


Figure 10. Cloud horizontal scale versus cloud bases and tops for 19 basic cloud scenarios used in the simulations of cloud effects on Shuttle imaging.

The small open rectangles in Figure 10 show 10 basic cloud scenarios with bases at 4000 ft, 8000 ft, 30 000 ft and 50 000 ft, Cloud thicknesses were specified at 500 ft over a range of horizontal scales from 1-to-32 n mi. These geometrically thin clouds were assumed to be optically thick, capable of obscuring a camera's view of the Shuttle. Cloud fraction was varied from 0/8 to 0/8 for these 10 scenarios. A ceiling, that is cloud cover of 5/8s or greater, at less than 4000 ft feet would be No Go for existing weather launch commit criteria (LCC), whereas a ceiling at 8000 ft or more would be GO for existing Weather LCC.

Ceilings between 4000 ft and 8000 ft can be waived under existing weather LCC. The 30 000 ft and 50 000 ft scenarios were selected to examine effects of cloud base height on viewing probabilities.

The large open rectangles in Figure 10 show 6 cloud scenarios with bases at 8000 ft and 30 000 ft, and with cloud thicknesses of 5000 ft. Cloud fraction was varied from 0/8 to 8/8 for these 6 scenarios. These geometrically thick clouds were also specified over a range of horizontal scales.

The solid bars in Figure 10 represent three scenarios with bases at 3000 ft and with vertical scales equivalent to their horizontal scales. These simulated clouds with 1:1 aspect ratios are representative of cumulus clouds that may be in the area during a launch. Simulations for these convective clouds were limited to coverages of 1/8 to 4/8 because greater coverage would constitute a 3000 ft ceiling and a No Go condition under existing weather LCC. Deeper convective clouds would likely be thunderstorms with lightning associated restrictions to launch.

For each of the cloud scenarios described above, 1000 trials were conducted with cloud element locations randomly assigned for each trial. The 1000 trials were made for each of 7 prescribed cloud coverages ranging from 1/8 to 7/8 by 1/8s. If adjacent cells were assigned as cloudy, then the cloud elements would effectively merge into a contiguous cloud. It was not necessary to simulate random trials for overcast conditions because the results were dependent only on the amount of time the Shuttle spent below cloud base and above cloud tops. Under clear conditions the Shuttle was assumed to be viewable 100% of the time from launch to SRB separation.

3.3 Method of Solution

An efficient numerical scheme was developed to determine if any cloud elements were in the LOS between each camera site and the Shuttle. The equation of the line connecting each camera and the Shuttle was computed in ECEF coordinates and used to determine if the line pierced any of the cloud elements within the relevant domain. This computation was done for each camera within the network and initially for each 0.1-second time interval during the ascent. Later testing indicated that a 0.5 second interval could be used without significantly affecting the results.

The method of solution can be described mathematically as follows:

To determine if a line, L , from O to S passes through a parallelepiped cuboid cloud, first define the six cloud faces by the intersections of the six planes $x = x_1$, $x = x_2$, $y = y_1$, $y = y_2$, $z = z_1$, $z = z_2$, where $x_1 < x_2$, $y_1 < y_2$, and $z_1 < z_2$, as shown in Figure 9

Represent the equation of the line L in vector form:

$$L = O + s \times (S - O),$$

where

$$s_i = (y_i - O_y) / (S_y - O_y)$$

and the subscript i represents one of the six faces. The other five faces could be represented by j , k , l , m , and n , respectively. Then compute

$$x_i = O_x + s_i \times (S_x - O_x), \text{ and}$$

$$z_i = O_z + s_i \times (S_z - O_z).$$

If $x_1 < x_i < x_2$ and $z_1 < z_i < z_2$, then L intersects the cloud face defined by plane $y = y_1$. If s_i is between 0 and 1, then the intersection falls between O and S . Solve the same set of equations and conditions for y_2 , x_1 , x_2 , z_1 , and z_2 . If L satisfies any of the conditions then L intersects the cloud element between O and S .

3.4 Model Output

Table 3 shows an example of model output for one of 1000 trials with cloud bases at 3000 ft cloud tops at ~ 9000 ft and a cloud cover of 1/8. The first column shows time after lift-off in seconds. The second

column shows a string of binary digits for clear views (0) and obscured views (1) for each of the camera sites listed in Tables 1 and 2 except for UCS-25, for a total of 21. Each camera has its own position within the binary string.

Table 3. Sample model output for 21 Medium and Long Range cameras. The first column shows time from lift-off in 0.5 second intervals. The second column shows a binary code that is explained in the text below.

| Time (seconds) | Binary Code (0 = Clear; 1= Obscured) |
|----------------|--------------------------------------|
| 0.0 | 00000000000000000000 |
| 0.5 | 00000000000000000000 |
| 1.0 | 00000000000000000000 |
| ↓ | ↓ |
| 10.0 | 00000000000000000000 |
| 10.5 | 01000000000000000000 |
| 11.0 | 01000000000000000000 |
| 11.5 | 01000000000000000000 |
| 12.0 | 01000000000000000000 |
| 12.5 | 01000000000000000000 |
| 13.0 | 11000000000000000000 |
| 13.5 | 11000000000000000000 |
| 14.0 | 11000000000000000000 |
| 14.5 | 11000000000000000000 |
| 15.0 | 11000000000000000000 |
| 15.5 | 11000000000000000000 |
| 16.0 | 11000000000000000000 |
| 16.5 | 11000000000000000000 |
| 17.0 | 11000000000000000000 |
| 17.5 | 11111111111111111111 |
| 18.0 | 11111111111111111111 |
| 18.5 | 11111111111111111111 |
| ↓ | ↓ |
| 29.5 | 11111111111111111111 |
| 30.0 | 00110111111111111111 |
| 30.5 | 00110111111111110111 |
| 31.0 | 00110111111111110111 |
| 31.5 | 00110111011110100111 |
| 32.0 | 00110110101101010011 |
| 32.5 | 00110110101101010011 |
| 33.0 | 00110001001010100111 |
| 33.5 | 00110001001010100111 |
| 34.0 | 0011000100101000111 |
| ↓ | ↓ |
| 124.0 | 001000111000101010100 |

The model output format shown in Table 3 was designed to facilitate the analysis of at least 3-simultaneous views for any combination of cameras within the pre-upgrade or post-upgrade camera networks. The first two binary digits in the second column of Table 3 are for the two airborne cameras. For this particular trial these cameras had a clear view of the Shuttle until 10.5 seconds after lift-off when one of them became obscured. Within a few seconds both airborne cameras were obscured. Recall that the airborne cameras were located at 65 000 ft altitude, 15 n mi NE and SW of the SRB separation point (see Fig. 4). At 17.5 seconds after lift-off all simulated cameras in the network lost sight of the Shuttle as it entered the base of a cloud element. At 30 seconds after lift-off the Shuttle emerged from the cloud top and was sighted by both airborne cameras and one of the ground based cameras near Launch Complex 46 (LC-

46). Within a few seconds after that most of the cameras in the network had clear views of the Shuttle. However, as the ascent continued, obscuration continued for some of the ground based cameras, ended for others, and came and went for some as the cameras slewed across the partly cloudy sky, tracking the Shuttle.

4. Analysis Results

4.1 Probability of at least 3 Simultaneous Views with Upgraded Camera Network

For each of 1000 trials of a given cloud scenario and cloud coverage, the model output was analyzed to determine the fraction of time from lift-off to SRB separation that the Shuttle was viewable simultaneously by at least 3 cameras. The average percentages were computed for cloud coverage ranging from clear to overcast by increments of 1/8.

Figure 11 shows fractional cloud coverage versus the percent of time from lift-off to SRB separation that the Shuttle was viewable simultaneously at least 1, 2 and 3 cameras in the upgraded network, including 2 airborne cameras. A mid-level cloud base at 8000 ft was chosen because of existing weather LCC. The weather LCC for Shuttle ceiling rules would be GO for a ceiling (cloud cover > 4/8) at or above 8000 ft. Figure 11 indicates that the percent of time the Shuttle is viewed simultaneously by at least 3 cameras decreases rapidly as cloud cover increases beyond 6/8. At the point where cloud cover reaches 7/8 the percent viewable factor has decreased to less than 80% for 3 cameras. However, for 2 cameras or 1 camera the percent viewable remains above 98% because the airborne cameras acquire the Shuttle as soon as it emerges from the top of the clouds, and the ground based cameras have an unobstructed view until the Shuttle enters the cloud base.

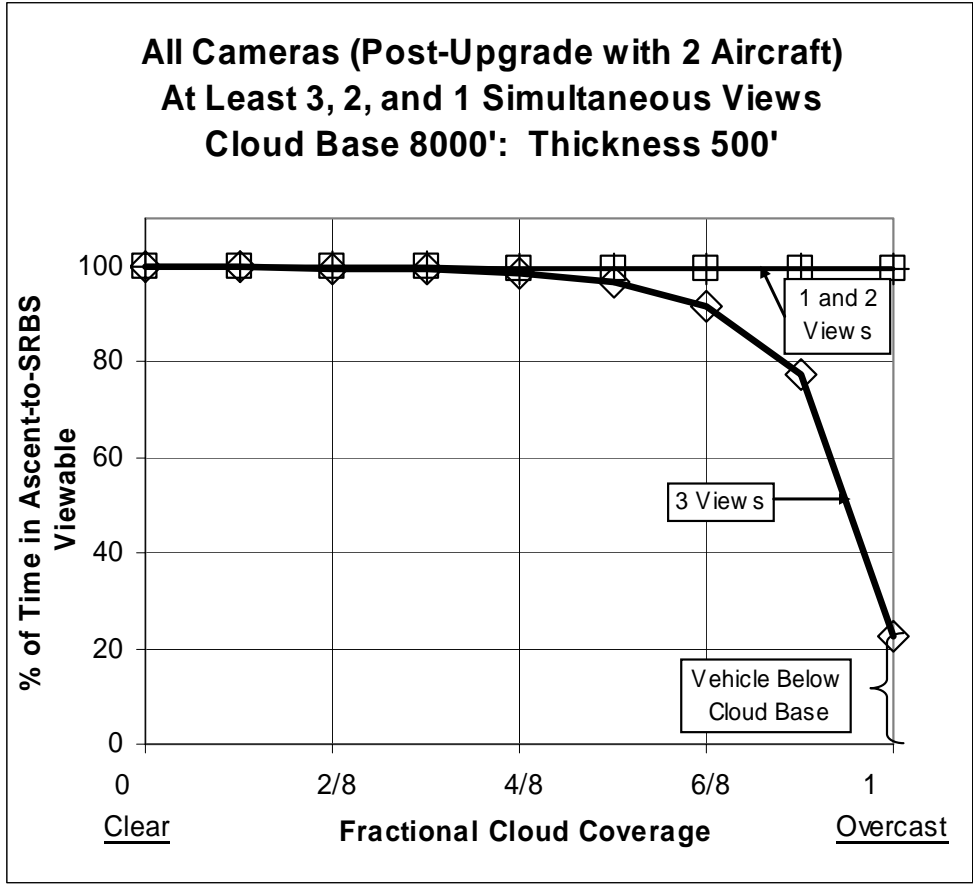


Figure 11. Fractional cloud cover versus % of time between lift-off and SRB separation that the Shuttle was viewable simultaneously by at least 1, 2 and 3 cameras.

4.1.1 Sensitivity to Cloud Base Height

Figure 12 shows fractional cloud coverage versus the percent of time between lift-off and SRB separation that the Shuttle was viewable simultaneously by at least 3 cameras in the upgraded network with 2 aircraft for cloud bases at 4000 ft, 8000 ft, and 30 000 ft, a cloud thickness of 500', and a cloud horizontal dimension of 4 n mi. For overcast conditions the percent of time viewable is greatest for the 30 000' case, simply due to the increased time that it takes the Shuttle to reach cloud base and to be obscured from the ground-based cameras for the remainder of the ascent. Once the Shuttle is above the overcast the 2 airborne cameras cannot satisfy the requirement for 3 simultaneous views. For cloud coverages of 6/8, and less the time viewable exceeds 90 % for the low, middle, and high cloud base examples used in the simulation.

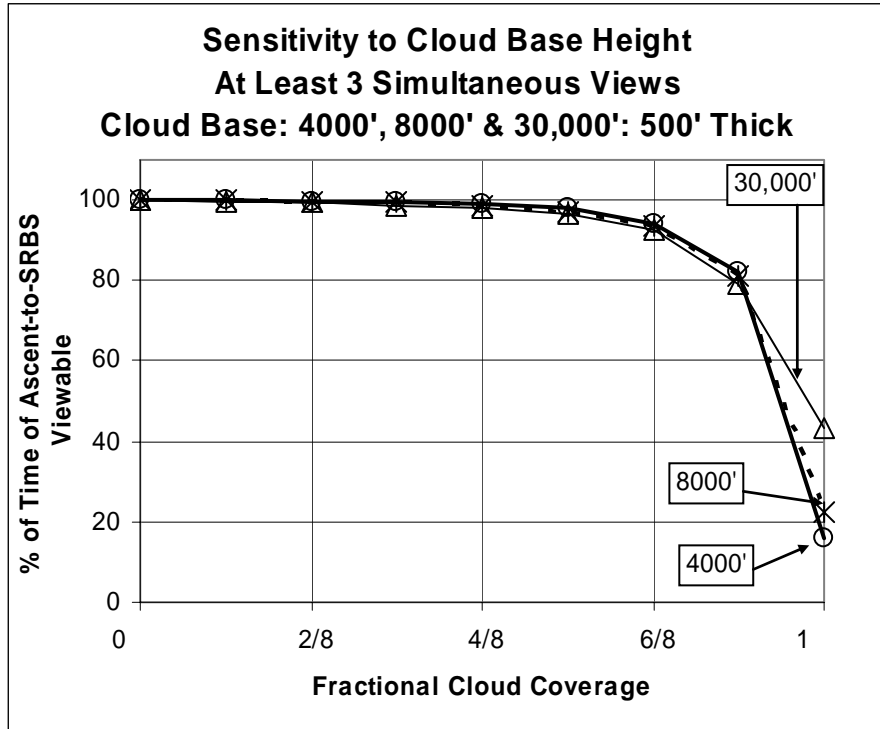


Figure 12. Fractional cloud cover versus % of time from lift-off to SRB separation that the Shuttle was viewable simultaneously by at least 3 cameras for cloud bases at 4000 ft, 8000 ft, and 30 000 ft.

4.1.2 Sensitivity to Cloud Thickness

Figure 13 shows fractional cloud coverage versus percent of time between lift-off and SRB separation viewable by at least 3 cameras, for cloud bases at 8000 ft and cloud thicknesses of 500 ft (solid curve) and cloud thicknesses of 5000 ft (dashed curve). It is evident that thick clouds are more efficient at obscuring views of the Shuttle than thin clouds due to 3D effects. The sides of thick clouds obscure a greater part of the sky than thin clouds, when viewed at elevation angles $< 90^\circ$.

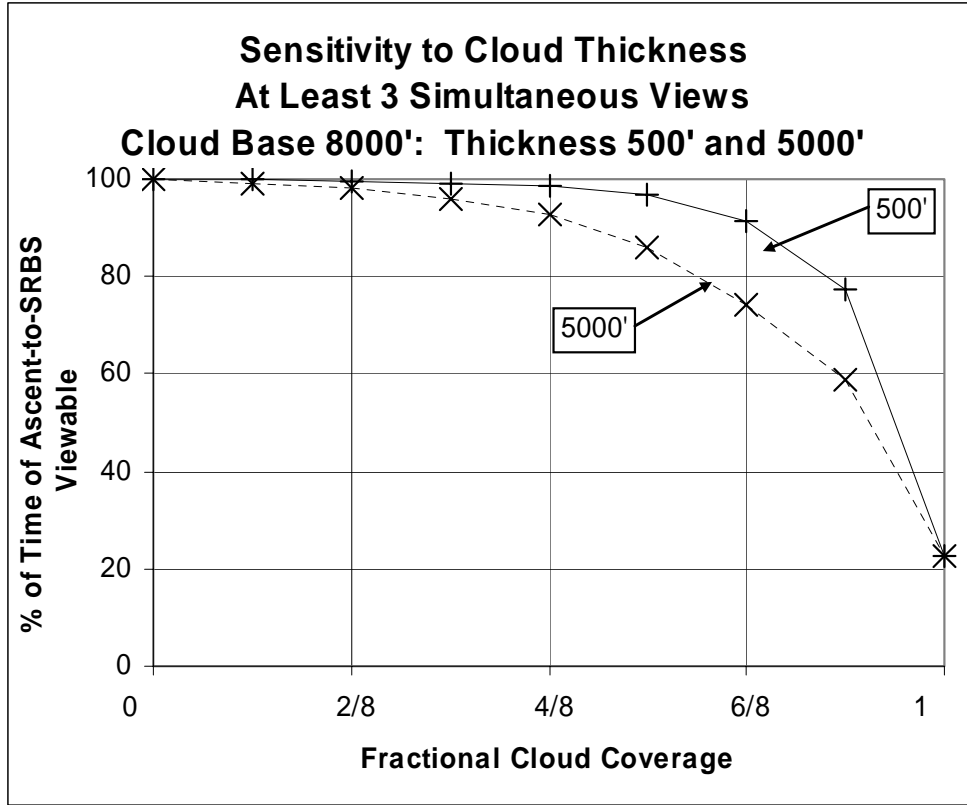


Figure 13. Fractional cloud cover versus % of time between lift-off and SRB separation that the Shuttle was viewable simultaneously by at least 3 cameras for cloud bases at 8000 ft and cloud thicknesses of 500 ft and 5000 ft.

4.1.3 Sensitivity to Cloud Horizontal Dimension

Figure 14 shows fractional cloud coverage versus percent of time between lift-off and SRB separation viewable by at least 3 cameras, with cloud bases at 8000 ft, cloud thicknesses of 500 ft, and horizontal dimensions of 1, 4 and 8 n mi. The thick solid curve is for a horizontal dimension of 1 n mi, the dashed curve is for a dimension of 4 n mi, and the thin solid curve is for a horizontal dimension of 8 n mi. The percent of time viewable was relatively insensitive to cloud horizontal dimensions over the range of 1 - 4 n mi. For a dimension of 8 n mi the percent of time viewable was lower for cloud coverages of 1/8 to 5/8. As cloud coverage increased toward overcast conditions the percent viewable time became less sensitive to the horizontal dimensions of the cloud elements.

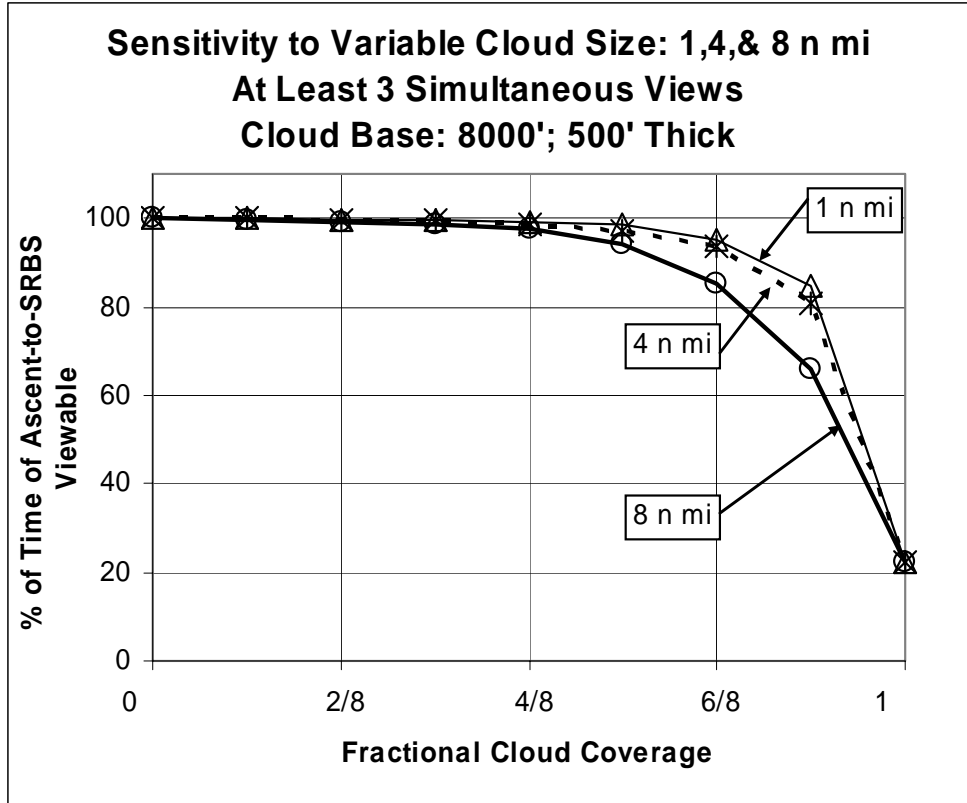


Figure 14. Fractional cloud cover versus % of time between lift-off and SRB separation that the Shuttle was viewable simultaneously by at least 3 cameras for cloud bases at 8000 ft, cloud thicknesses of 500 ft and cloud horizontal dimensions of 1, 4, and 8 n mi.

4.1.4 Sensitivity to Cloud Layering

Figure 15 shows fractional cloud coverage versus percent of time between lift-off and SRB separation viewable by at least 3 cameras, for two cases: One with cloud bases at 8000 ft, and the other with cloud bases at 8000 ft and 30 000 ft. Both cloud layers have thicknesses of 500 ft, and horizontal dimensions of 8 n mi. The solid curve is for the case with 8000 ft cloud bases only and the dashed curve is for the 2-layer case. Fractional cloud coverage for each layer was incremented simultaneously, from clear to overcast by 1/8s. The random placement of cloud elements in the 2-layer case was independent. As a result, the fractional cloud coverage of the 2-layer case, defined as the fraction of cells in the model domain occupied by cloud elements, was calculated by taking into account the average random overlapping of cloud elements in the two layers. The percent of time viewable was slightly higher for the 2-layer case when the fractional cloud coverage was in the range from 6/8 to almost overcast.

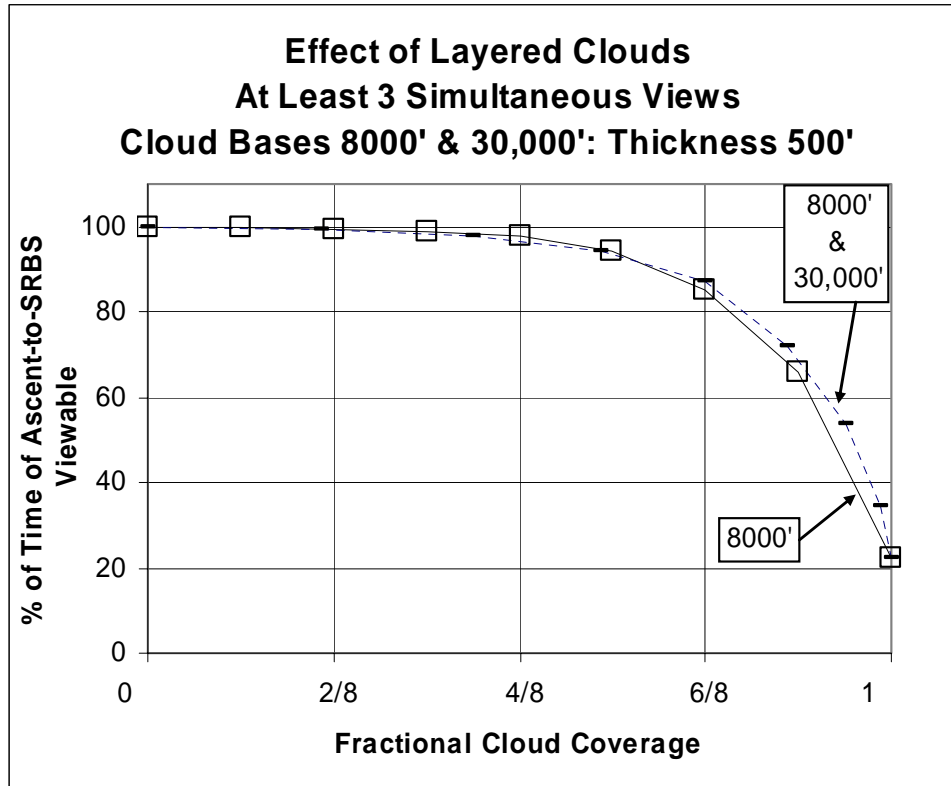


Figure 15. Fractional cloud cover versus % of time between lift-off and SRB separation that the Shuttle was viewable simultaneously by at least 3 cameras for two cases: Cloud bases at 8000 ft, cloud thicknesses of 500 ft and cloud horizontal dimensions of 4 n mi (thin line), and cloud layers at 8000' and 30 000 ft with the same thicknesses and horizontal dimensions.

4.2 Comparison of Post- and Pre- Upgraded Networks

Figure 16 shows the average percent of time between lift-off and SRB separation that the Shuttle was viewable simultaneously by at least 3 cameras for the pre-upgrade configuration (Δ), the post-upgrade configuration without airborne cameras (O) and the post-upgrade configuration with airborne cameras (*). Cloud coverage varied from clear to overcast, with cloud bases at 8000 ft and cloud tops at 8,500 ft. Under clear conditions the pre-upgrade and post-upgraded networks provided at least 3 simultaneous views 100 % of the time, as expected. However, at 4/8 cloud cover the pre-upgrade configuration provided at least 3 simultaneous views only 59% of the time, compared to 90% for the post-upgrade with airborne cameras and > 98% for the post-upgrade with airborne cameras. Under clear conditions all three network configurations provided at least 3 simultaneous views 100 % of the time from any combination of cameras within the network. As cloud cover increased the performance of the pre-upgrade configuration decreased rapidly, whereas the post-upgrade configuration showed a percent viewable factor greater than 90% out to a cloud coverage of 4/8. When airborne cameras were added to the post-upgrade configuration, the 90% performance level was maintained out to 6/8 cloud coverage. For overcast conditions the percent viewable factor decreased to ~ 22% because that is the time the Shuttle spends below the cloud deck. Once above the cloud deck there are only two airborne cameras and the ground-based optical imaging systems are obscured by clouds.

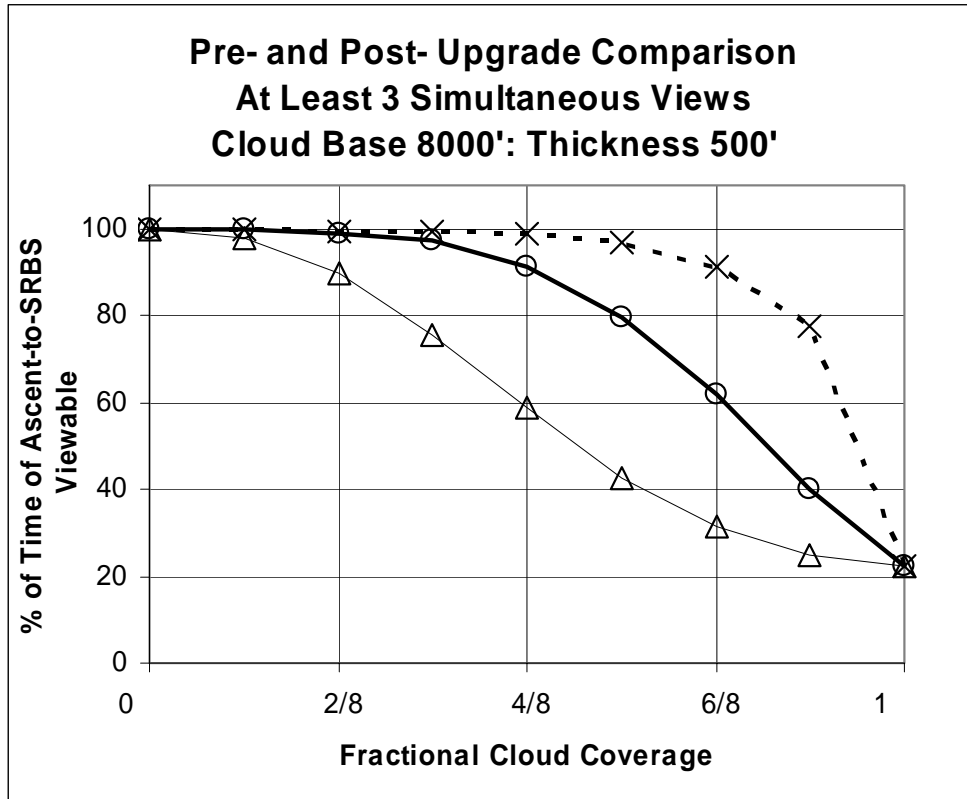


Figure 16. Fractional cloud cover versus % of time between lift-off and SRB separation that the Shuttle was viewable simultaneously by at least 3 cameras for the pre-upgrade network (Δ), the post-upgrade network without airborne cameras (O), and the post-upgrade network with airborne cameras (*), for cloud bases at 8000 ft, and cloud thicknesses of 500 ft.

Figure 17 shows the average percent of time between lift-off and SRB separation that the Shuttle was viewable simultaneously by at least 3 cameras for the pre-upgrade configuration (Δ), the post upgrade configuration without airborne cameras (O and o) and the post-upgrade configuration with airborne cameras (* and *), as cloud coverage varied from clear to overcast, with cloud bases at 8000 ft and cloud tops at 8,500 ft. The small symbols (o and *) with thin lines for the post-upgrade network denote configurations where the total number of ground-based long range cameras was reduced from 10 to 8. The effect of dropping two ground-based cameras is very small when the two airborne cameras are included. For the case with the post-upgraded network without airborne cameras the effect is somewhat greater. For example, with 4/8 cloud cover the % of time viewable drops when 90% to 85% when the total number of long-range cameras is reduced from 10 to 8.

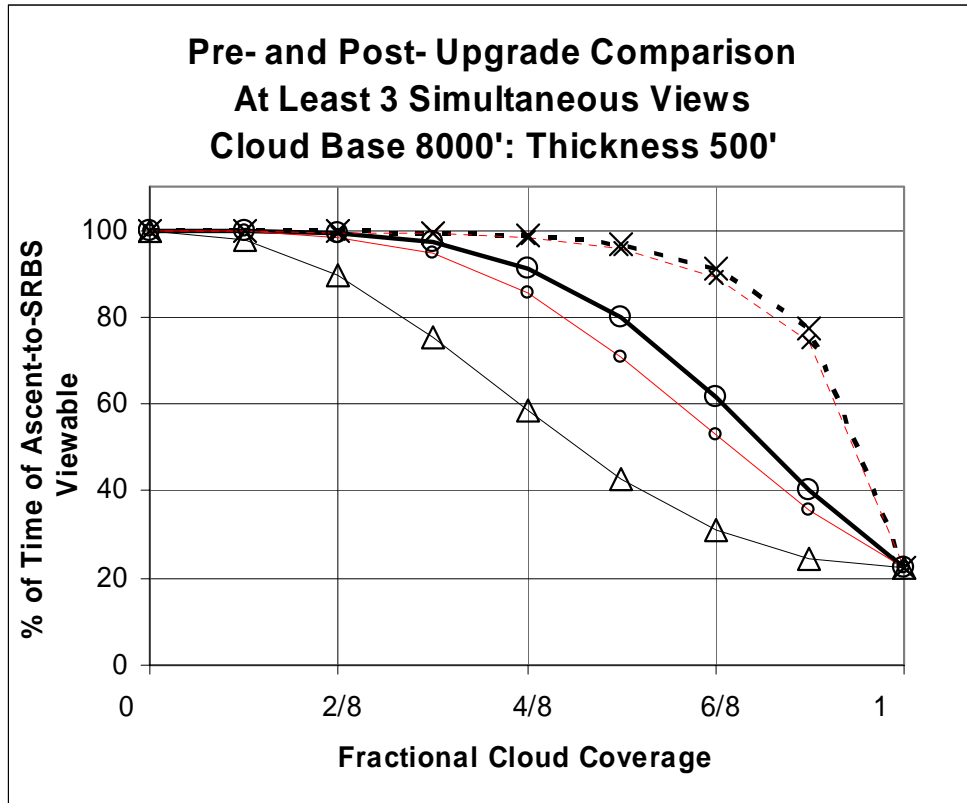


Figure 17. Fractional cloud cover versus % of time between lift-off and SRB separation that the Shuttle was viewable simultaneously by at least 3 cameras for the pre-upgrade network (Δ), the post upgrade network without airborne cameras (O and o), and the post-upgrade network with airborne cameras (* and *), for cloud bases at 8000 ft, and cloud thicknesses of 500 ft. The small symbols denote a change in the post-upgrade configuration from 10 to 8 long-range cameras.

5. Summary

5.1 Objective

The objective of this study was to obtain a quantitative description of the effect of cloud obscuration on optical imaging of the Shuttle between lift-off and SRB separation by a network of ground-based and airborne cameras. The AMU was tasked by the KSC Weather Office to develop a 3D simulation model and analyze its output in order to meet the objective. The overall effort was motivated by a recommendation (R3.4-1) from the CAIB Report for Space Shuttle RTF that called for an upgrade of the imaging system to be capable of providing a minimum of three useful views of the Shuttle from liftoff to at least solid rocket booster separation, along any expected ascent azimuth. Ships or aircraft were to be considered for providing additional views of the Shuttle.

5.2 Camera Network, Ascent Trajectory and Line-of-Sight data

The AMU obtained the latitude/longitude coordinates of camera sites in the network and camera capabilities from the NASA IWPG. The network configurations prior to and after upgrade were also provided. An ascent trajectory from SLC-39B to the ISS was selected because the missions after Return-to-Flight are expected to be to the ISS. The AMU computed the LOS from each camera to the Shuttle for each camera location and each Shuttle position in the trajectory at 0.1 second intervals. Later analyses revealed that the LOS time interval could be lengthened to 0.5 seconds without affecting the results of the study.

5.3 Simulation Model and Cloud Scenarios

A statistical approach using an idealized simulation model was selected by a Team composed of the Shuttle Launch Director, The NASA IPWG, the KSC Ice and Debris Team, the KSC Weather Office, the 45 WS and the AMU for determining the effect of clouds on Shuttle imaging. The idealized statistical approach was chosen because it was found by Bauman (2003) that current instrumental and modeling capabilities do not permit sufficiently accurate observations and forecasts of real cloud morphology and location to warrant the expense required for such an effort. The Shuttle LWO and the KSC Weather Office provided guidance on a variety of operationally significant cloud scenarios for use in the simulation model.

The AMU formulated a 3D simulation model and randomly populated it with idealized opaque clouds for each simulated ascent. The camera network and a Shuttle ascent trajectory to the ISS were embedded in the 3D model and the LOS data was then used to determine how many cameras simultaneously had a clear view of the Shuttle at each 0.5 second interval from lift-off to SRB separation in the presence of clouds. For each cloud scenario 1000 simulation trials were conducted and the average percent of time viewable simultaneously by 3 cameras was computed. Characteristics of the cloud population such as cloud base, height, thickness, horizontal dimension and fractional coverage were varied systematically from one scenario to the next. Cloud locations were varied randomly from one simulation trial to the next within a given scenario.

Analyses of the percent of time viewable were made to determine its sensitivity to cloud amount, cloud base height, cloud thickness, cloud horizontal dimensions, and the upgrade of the camera system.

5.4 Results

The average percent of time viewable was found to be most sensitive to fractional cloud cover, as expected. For overcast conditions the recommendation for at least 3 simultaneous views could only be met while the Shuttle was below cloud base. For a high overcast of cirrus clouds with bases at 30 000 ft the percent of time viewable would be less than 50%. Broken cloud cover, that is 5/8 to 7/8 coverage, generally would allow 80% or less viewable time, without airborne cameras. The airborne cameras increase the probability of 90% or better time viewable with at least three cameras simultaneously up to about 6/8 cloud coverage.

Upgrades in the camera network had significant impacts on the average percent of time viewable. The impact of upgrading the ground-based network was found to be roughly equivalent to decreasing the cloud cover by about 2/8 in terms of the increased percent of time viewable, except for overcast conditions as noted above. The addition of airborne cameras was roughly equivalent to decreasing the cloud cover by about 4/8, except for overcast conditions.

Sensitivity to other variables was less significant. Cloud elements with horizontal dimensions larger than about 4 n mi were more efficient in reducing the percent time viewable by 3 cameras simultaneously, presumable because larger clouds were more efficient at obscuring the views of more than one camera at a time. Thicker clouds were also found to be more efficient at reducing the percent of time viewable, because at the typical viewing angles, < 60° above the horizon, the effective cloud cover is increased by the sides of the clouds. An increase in cloud thickness from 500 ft to 5000 ft was roughly equivalent to increasing the fractional cloud cover by 1/8 to 2/8.

5.5 Future Work

The geographic boundaries of the domain where clouds could potentially obscure imagery of the Shuttle from network cameras are dependent on the camera locations, the launch trajectory and the heights of cloud bases and tops. A software tool for plotting the boundaries could be used to provide subjective operational guidance to the Shuttle LWO regarding the susceptibility of various camera sites to cloud obscuration in real-time, if it were developed into an overlay for satellite imagery.

6. Bibliography

Bauman, W. H., III, 2003: Shuttle imaging weather evaluation concept study. Applied Meteorology Unit Memorandum. [Available from ENSCO, Inc., 1980 N. Atlantic Ave., Suite 230, Cocoa Beach, FL 32931]

National Aeronautics and Space Administration, 2003: Columbia Accident Investigation Board Report: Volume I. Government Printing Office, Washington D.C., 248 pp.

Paté-Cornell, M.-E., and P. S. Fischbeck, 1994: Risk management for the tiles of the space shuttle. *Interfaces*, **24**, 64-86.

List of Acronyms

| | |
|-------|---|
| 45 WS | 45th Weather Squadron |
| AMU | Applied Meteorology Unit |
| CAIB | Columbia Accident Investigation Board |
| CB | Cloud Base |
| CT | Cloud Top |
| ECEF | Earth Centered Earth Fixed |
| ISS | International Space Station |
| IPWG | Intercenter Photo Working Group |
| KSC | Kennedy Space Center |
| LC | Launch Complex |
| LCC | Launch Commit Criteria |
| LOS | Line-of-Sight |
| N | Number |
| NASA | National Aeronautics and Space Administration |
| RTF | Return-to-Flight |
| SRB | Solid Rocket Booster |
| STS | Space Transportation System |
| UCS | Universal Camera Site |

NOTICE

Mention of a copyrighted, trademarked, or proprietary product, service, or document does not constitute endorsement thereof by the author, ENSCO, Inc., the AMU, the National Aeronautics and Space Administration, or the United States Government. Any such mention is solely for the purpose of fully informing the reader of the resources used to conduct the work reported herein.